

High-Performance dc SQUID Sensors and Electronics

D. Drung^{a)}, C. Aßmann^{a)}, J. Beyer^{a)}, A. Kirste^{a)}, M. Peters^{a)}, F. Ruede^{a)}, Th. Schurig^{a)}, C. Hinnrichs^{b)}, and H.-J. Barthelmeß^{b)}

^{a)} Physikalisch-Technische Bundesanstalt, Abbestr. 2-12, 10587 Berlin, Germany

^{b)} Magnicon GbR, Lemsahler Landstr. 171, 22397 Hamburg, Germany; e-mail:

barthelmeß@magnicon.com

Abstract—We introduce a new family of low-noise, robust, and easy-to-use dc SQUID sensors for a wide range of applications. In combination with our high-performance dc SQUID read-out electronics and a state-of-the-art packaging and wiring of the sensors, we obtain complete solutions for established measurement tasks as well as for new application concepts. For the readout of transition-edge sensors (TESs), series arrays of 16 gradiometric SQUIDs are fabricated which can be mounted directly on a Cu block at the cold stage of a mK cryostat without degradation in noise. Integrated two-stage sensors consisting of a single front-end SQUID with a double-transformer input coupling read out by a 16-SQUID series array are developed for applications requiring a high input inductance of up to 1.8 μH and an ultra-low current noise down to 180 $\text{fA}/\text{Hz}^{1/2}$ at 4.2 K. Single-stage SQUIDs with additional positive feedback (APF) and bias current feedback (BCF) were implemented for applications with relaxed demands on the SQUID noise. For magnetic sensing field applications (e.g. monitoring of environmental interferences), integrated miniature multiloop magnetometers were designed with maximized field resolution. For a 3 mm \times 3 mm chip size, a noise level below 4 $\text{fT}/\text{Hz}^{1/2}$ is obtained at 4.2 K. In this paper, we report about latest developments of our SQUID sensors, SQUID electronics, and sensor packaging.

Manuscript received June 25, 2007; accepted in final form on June 26, 2007; reference No. (ST2)

I. INTRODUCTION

Superconducting quantum interference devices (SQUIDs) are used in a wide range of applications as magnetic flux detectors and current sensors. In applications like X-ray astronomy (microcalorimeters, bolometers) and energy dispersive X-ray analysis (EDX) the read-out of transition-edge sensors (TESs) using SQUIDs demands a high dynamic performance and insensitivity to external magnetic fields at moderate input inductances in the range of some nH. However, applications like biomagnetism (magnetoencephalography, magnetorelaxometry), nuclear magnetic resonance (NMR), and susceptometry require ultimate noise performance with input inductances in the μH range. For applications like environmental noise characterization, low-noise magnetometers capable to be cooled in the Earth magnetic field without degradation of noise performance are needed. Additionally, some of these applications require the operation of the SQUID sensors at temperatures far below the temperature of liquid Helium (4.2 K), down to some mK. To provide the best possible sensor performance for nearly all kinds of measurement tasks, we developed a new family of SQUID sensors including single-stage current sensors, integrated two-stage current sensors, SQUID series arrays [1], and magnetometers offering a large range of parameters [2]. To utilize the performance of the different sensors, the development of new sensor packaging and wiring was necessary.

To operate this variety of sensors, a fully computer-controlled, flexible high-performance dc SQUID electronics (XXF-1) was developed [3]. This electronics offers on-board features to operate two-stage devices, TESs, and SQUID arrays. Due to the high maximum flux-locked-loop (FLL) bandwidth of 20

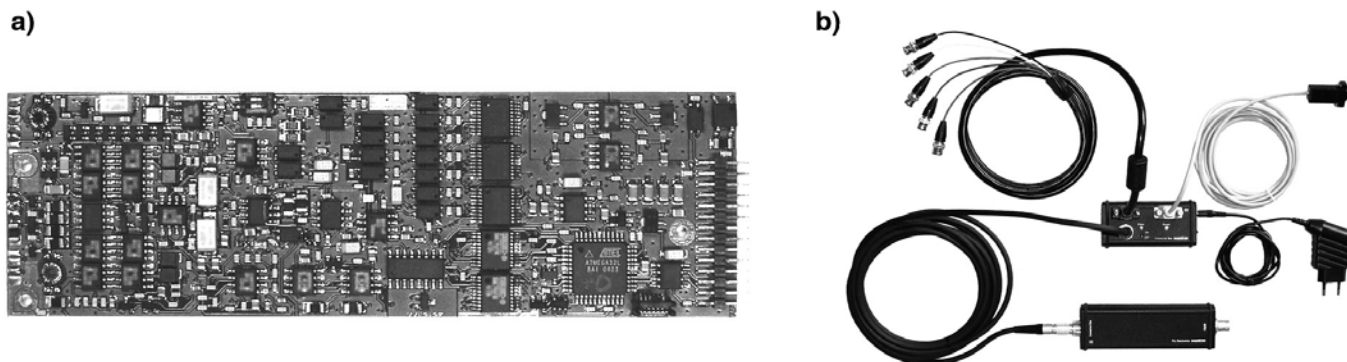


Fig.1. Photograph of a) one FLL board with size 13 cm \times 4.3 cm and b) of the complete electronics system with FLL electronics unit, connector box, output cable, optically isolated RS-232 connection cable, and power supply.

MHz [4,5], and perfect matching of electronics and sensors, an easy-to-use and reliable solution for a wide range of applications can be offered.

Here, we describe our latest developments in SQUID electronics, SQUID sensors, and packaging.

II. DC SQUID ELECTRONICS

A. Basic Features of Electronics

A photograph of the FLL board and of the complete electronics system (XXF-1) is shown in Fig.1a and Fig.1b, respectively. A total of 670 surface-mount components are placed on both sides of the 13 cm \times 4.3 cm FLL board. Up to three FLL boards can be mounted in one aluminum case to build a compact three-channel system. The FLL unit is commonly placed at the top of the cryostat to minimize the distance between the SQUID sensor and the readout electronics. It is connected to a so-called connector box via a shielded cable containing several 50 Ω coaxial lines and control wires. The connector box makes the FLL output accessible to the user and provides the system power.

The FLL board contains all circuits needed to operate the SQUID. It includes an in-system programmable microcontroller, 10 digital-to-analog converters and 49 electronic analog switches for generating the SQUID bias signals and for setting the system parameters. The output signal is available in analog form (± 10 V voltage range). However, some basic parameters like the board temperature, preamplifier input voltage and electronics output voltage are monitored via integrated 10-bit analog-to-digital converters. To adapt the electronics to the particular sensor application and to the parameters of the SQUID in use, the feedback resistance can be chosen between 0.7 and 100 k Ω , and the gain–bandwidth product can be varied between 230 MHz and 7.2GHz in steps of about 1.7 dB. For optimum dc performance, circuits were included to eliminate the preamplifier offset voltage and current, and to minimize the temperature drift of the offsets. The electronics also feature a built-in SQUID heater circuit, an external flux input, and an external reset input, which allows one to reset the integrator in less than 1 μ s. The latter feature is particularly useful for pulsed applications such as NMR or magnetorelaxometry. A wide bias voltage range of 1.3 mV makes possible the readout of series SQUID arrays. For the readout of transition-edge sensors (TESs) or two-stage SQUIDs, the electronics is equipped with two additional integrated current sources. In TES applications, one source is used to generate the bias current of the TES while the other provides calibration pulses with a duration selectable between 1 μ s and 2 ms. In two-stage

SQUID applications, the additional current sources are used to generate the bias current of the front-end SQUID and the bias flux of the second stage (single SQUID or series SQUID array). An optional feedback path around the second stage allows visualization of the flux-to-voltage characteristics of the front-end SQUID without changing the wiring.

The modular concept of the LabVIEW[®] based Windows[®] software SQUIDViewer[™] allows easy access and adjustment of all electronics parameters. With two integrated waveform generators, all current and voltage sources in the electronics can be modulated with a variety of waveforms to allow sensor characterization and testing without the need of external sources. Other useful features are convenient heater automatic and optional overload detection with automatic integrator reset. Additional PC boards with current sources and amplifiers can be integrated easily into the aluminum box and controlled by the software to allow operation of multiple TESs and auxiliary coils together with the SQUID electronics.

B. Preamplifier Performance

In order to achieve excellent dc precision and a high amplifier bandwidth simultaneously (a prerequisite for wideband FLL electronics without flux modulation), we developed a composite preamplifier consisting of a slow but precise dc amplifier in parallel with a fast ac amplifier. The outputs of both amplifiers are summed via an R - C network with a crossover frequency $f_0 \approx 80$ Hz. Two filters are placed at the amplifier inputs: an L - R low-pass at the dc amplifier and an R - C high-pass at the rf amplifier. This prevents mutual distortion of the amplifiers and removes current noise outside the respective useful frequency band.

Fig.2a shows the reduced small-signal frequency response of the amplifier gain (*i.e.*, the frequency-dependent gain divided by the dc gain) for source resistances R_S of 1 Ω , 50 Ω , and 10 k Ω . Even at the highest source resistance of 10 k Ω there is no significant change in the frequency response up to the cut-off frequency of about 50 MHz. These data are measured in the so-called amplifier (AMP) mode where the feedback electronics act as an amplifier with an adjustable gain between 1100 and 2000. This mode is also used for recording the SQUID characteristics. The preamplifier noise performance from 0.1 Hz to 100 MHz is depicted in Fig.2b and Fig.2c. The voltage and current noise spectra were measured using a source resistance of 1 Ω and 10 k Ω , respectively. In order to obtain the true input-referred amplifier noise, we subtracted the analyzer noise from the measured output noise, divided the result by the corresponding frequency response (Fig.2a), and subtracted the Nyquist noise in the source resistance (0.13 nV/Hz^{1/2} for the voltage noise and 1.3 pA/Hz^{1/2} for the current noise). Very low white and $1/f$ noise levels are achieved: 0.33 nV/Hz^{1/2} and 2.6 pA/Hz^{1/2} in the white noise regime above 1 kHz, and 0.8 nV/Hz^{1/2} and 40 pA/Hz^{1/2} at 0.1 Hz.

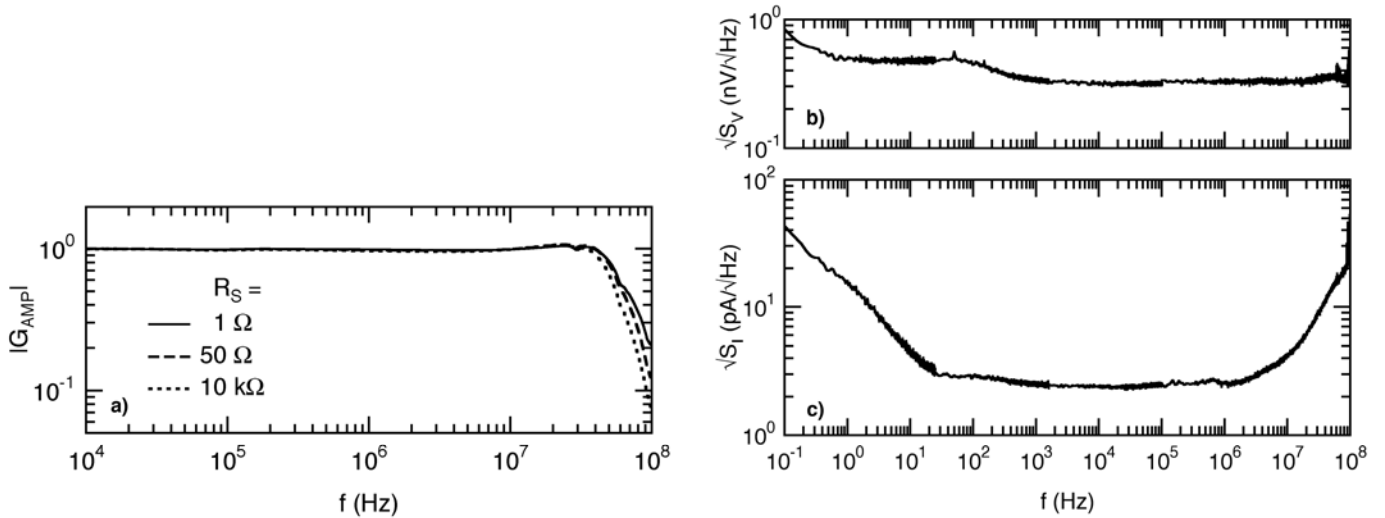


Fig.2. a) reduced small-signal frequency response of the amplifier gain in AMP mode for three different source resistances R_S . b) voltage and c) current noise spectra measured using a source resistance of 1Ω and $10 \text{ k}\Omega$, respectively.

III. SQUID SENSORS

A. Single-stage and Two-stage SQUID Current Sensors

In applications where ultimate noise performance is needed down to mK temperatures, two-stage SQUIDs are preferably used with a second SQUID acting as a low-noise preamplifier [5, 6]. The main parameter of a two-stage SQUID is the small-signal flux gain $G_\Phi = \partial \Phi_{amp} / \partial \Phi$ at the working point W. It specifies how much flux $\partial \Phi_{amp}$ is coupled into the amplifier SQUID if the flux in the front-end SQUID is changed by a small amount $\partial \Phi$. The contribution of the amplifier SQUID to the overall flux noise decreases with increasing the flux gain. Consequently, a high flux gain and a low flux noise of the amplifier SQUID (including contributions from the room temperature amplifier) are desirable. In our devices, additional positive feedback (APF) is used to increase the flux gain at the working point [5]. As the flux noise density S_Φ of series SQUID arrays decreases with the number of SQUIDs, they are nearly ideal preamplifiers [7], [8].

Figure 3 shows the design and simplified circuit diagram of our integrated two-stage sensor. The front-end SQUID is a second-order parallel gradiometer. Feedback, APF and input flux are coupled into separate washers in order to minimize the coupling between feedback/APF and input. For our latest sensors family, the variation in the feedback coil mutual inductance is only below 1% for the extreme cases of open and shorted input coil. The amplifier stage is a shunted 16-SQUID array with a parasitic area as low as about $1 \mu\text{m}^2$ in all field directions – corresponding to a field sensitivity of $2 \text{ mT}/\Phi_0$. This guarantees a constant flux bias of the array SQUIDs independent of magnetic background and thermal cycling. All SQUIDs on the chip are gradiometers in order to minimize their sensitivity to magnetic fields. A maximum cooling field on the order of $60 \mu\text{T}$ insures unshielded cool-down and operation in the Earth field. An additional feedback transformer in series to the input coil allows one to null the input current rather than the flux in the SQUID if desired [9]. To protect the input coil from large currents, an optional on-chip current limiter (Q-spoiler) may be used. It is a series array of 16 unshunted 20 pH SQUIDs connected in series with the input coil.

The white current noise level of the two-stage devices at 4.2 K , with the input coil open, is as low as $180 \text{ fA}/\text{Hz}^{1/2}$ for $1.8 \mu\text{H}$ inductance, corresponding to a coupled energy resolution of 44 h . With shorted input coil, the energy resolution improves by about one-third. When cooling the device to 300 mK , the

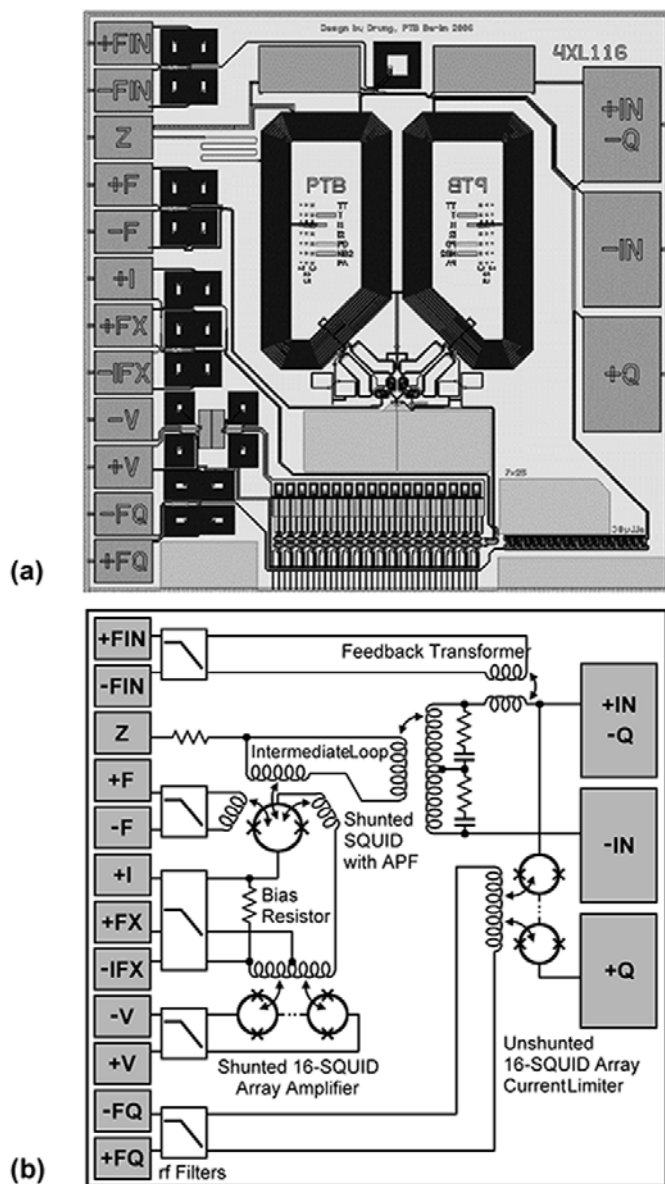


Fig.3: a) Layout and b) basic circuit diagram of the integrated two-stage sensor C4XL116. Chip size is 3 mm \times 3 mm. Circuit details (shunt resistors etc.) are omitted for clarity. Z is a test point for detecting shorts between the intermediate loop and the front-end SQUID or the input coil.

and 1.8 μ H are included on our latest mask set. The input inductance is varied by changing the number of turns in the input transformer between 8 and 80 turns, while keeping the total inductance of the intermediate loop roughly constant. In addition to the integrated two-stage devices, single-stage SQUIDs with APF and bias current feedback (BCF) [11] were implemented for applications with relaxed demands on the SQUID noise. The single stage sensors offer all basic features as described for the integrated two-stage devices like the Q spoiler, additional feedback transformer, integrated heating possibility, and minimized coupling between feedback/APF and input.

energy resolution drops to about 4 h. To simplify working point adjustment of the two-stage devices, the design provides user-friendly single-SQUID-like overall V - Φ characteristics [2].

All lines connecting the sensor chip with the room temperature readout electronics are passed through on-chip rf filters. The two-stage device requires a minimum of seven wires between room temperature and cryogenic part, *i.e.*, only two extra wires compared to a single-stage device. Only the three wires between the sensor output ($\pm V$ in Fig.3 plus one ground connection) and the room temperature preamplifier have to have a low resistance below a few Ohms [10]. Another attractive feature is that no separate heater resistor (and consequently no extra wire) is needed to expel trapped magnetic flux. In our setup the heater current is directly sent through the SQUID array. If the chip is immersed in liquid helium, an average power density of about 1 W/cm² (*i.e.*, about 0.1 W for our 3 mm \times 3 mm chips) is sufficient to heat up the complete chip above the critical temperature of the Nb films. Obviously, in vacuum the required heating power is lower. During the heating process, the voltage drop across the SQUID array is typically 5 V. Thus, the preamplifier has to be disconnected while heating. The XXF-1 electronics (see Sec. II) contains all circuitry needed including a convenient optional heater automatic to disconnect the preamplifier and to set all current and voltage sources to zero while heating. The heating time can be set between 1 ms and 65 s [10].

A total of 23 different double-transformer SQUIDs with input inductances between 24 nH

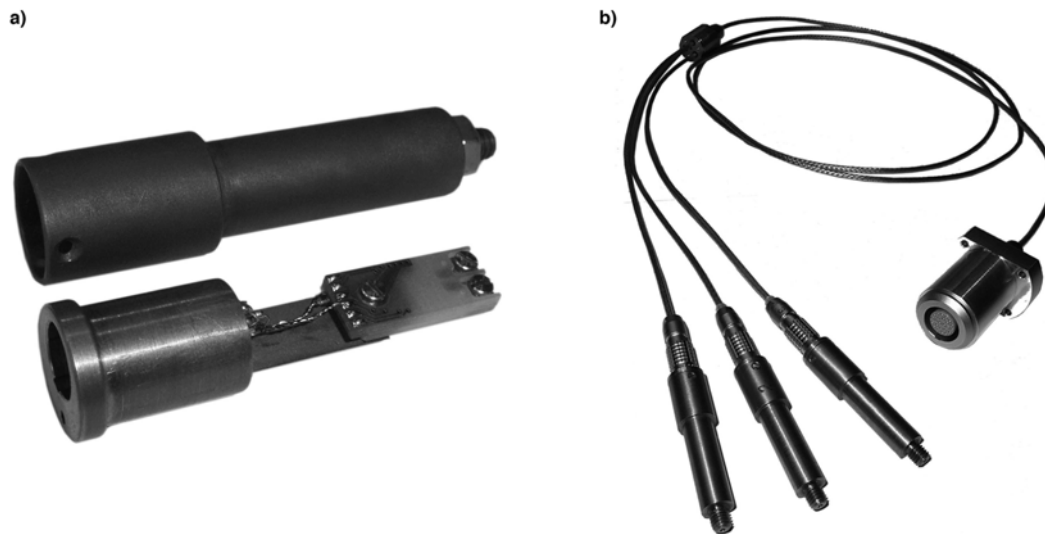


Fig.4. Photograph of a) chip carrier mounted on the Brass lid of the niobium can and b) cryocable with three connected niobium shielding cans.

B. SQUID Array Sensors

We have designed a series of low-inductance sensors for the readout of cryogenic detectors or for use as second stage in discrete two-stage setups. One $3 \text{ mm} \times 3 \text{ mm}$ chip contains two independent 16-SQUID series arrays. Each array has a feedback coil and an input coil with $L_{\text{in}} \approx 3 \text{ nH}$. For convenience, rf filters as well as bias resistors for detector operation were integrated into the chip. We have provided bias resistors of about 1Ω for two-stage setups, and bias resistors with nominal values of $90 \text{ m}\Omega$, $4 \text{ m}\Omega$ and $0.3 \text{ m}\Omega$ for detector readout. A current noise level $\leq 10 \text{ pA/Hz}^{1/2}$ is reached at a temperature of 4.2 K . The current noise decreases to $\leq 5 \text{ pA/Hz}^{1/2}$ when operating the devices at typical working temperatures of TESs ($\approx 100 \text{ mK}$), limited by the preamplifier noise contribution of the XXF-1 electronics [3]. For applications requiring a better energy resolution at low temperatures (at the expense of a reduced slew rate) we have realized two-stage sensors without input transformer. These devices have a lower input inductance of about 2 nH , and an improved current noise level of $6 \text{ pA/Hz}^{1/2}$ at 4.2 K or $2 \text{ pA/Hz}^{1/2}$ at 300 mK . Our SQUID arrays are very robust and insensitive to magnetic fields. They can be cooled down in the Earth field and may be mounted directly on a Cu block at the cold stage of a mK cryostat without degradation in noise. Their power consumption of $\approx 1 \text{ nW}$ per channel is acceptable in most applications. They are particularly interesting for applications where maximum dynamic performance is needed.

SQUID Magnetometers

We have also designed a few magnetic field sensors for applications where the large chip size ($7.2 \text{ mm} \times 7.2 \text{ mm}$) of our “biomagnetic” multiloop magnetometers W9L [5] is undesirable or a higher dynamic range is needed. In order to allow direct readout, APF and BCF were integrated on-chip similarly as in [11]. Stripline “spokes” have been used rather than coplanar “spokes” in order to maximize the field sensitivity [12]. A flux noise level of $1.2 \mu\Phi_0/\text{Hz}^{1/2}$ is achieved at 4.2 K , corresponding to 3.6 or $8.4 \text{ fT/Hz}^{1/2}$ for the devices with 2.8 mm or 1.7 mm outer pickup coil dimension, respectively. Considering the small loop size, the devices are very sensitive and useful for many applications.

IV. SENSOR PACKAGING

To offer a complete, reliable, and easy to use solution for different applications we have developed a small package for our new sensor family. It includes the chip carrier, niobium shielding can, and a cryocable, all shown in Fig.4. The chip carrier with outer dimensions of $7.1\text{mm} \times 18.1\text{mm} \times 3\text{mm}$ has screw terminals for superconducting connection to a pick-up coil. If our ultra-low noise two-stage sensors are used, the usually applied metal screws are replaced by screws out of a non-metallic material. This is necessary because metallic parts near the input circuit would increase the overall noise of the sensor.

The chip carrier can be mounted inside a superconducting niobium shielding can with an overall length of 56 mm and a maximum outer diameter of 12.7 mm. The capsule is equipped with a plug socket for easy connection to the cryocable. The superconducting wires to connect, *e.g.*, a pick-up coil can be fed through holes on both ends of the capsule depending on the situation inside the dewar. Additional external and internal threads allow easy mounting of the capsule.

The cryocable is fully screened with a stainless-steel braid. A flange at the warm side, holding the 24 pin LEMO plug for the SQUID electronics connection, permits vacuum-tight mounting on top of the dewar. Up to three niobium capsules can be connected to one cryocable via simple plug connections.

ACKNOWLEDGMENT

This work was partially supported by Investitionsbank Berlin (IBB), the German Federal Ministry of Economics and Technology (BMW), and the European Union (EU).

REFERENCES

- [1] R. P. Welty and J. M. Martinis, *IEEE Trans. Magn.* **27**, pp. 2924-2926, 1991.
- [2] D. Drung, C. Aßmann, J. Beyer, A. Kirste, M. Peters, F. Ruede, and Th. Schurig, Paper 5EB01, *IEEE Trans. Appl. Supercond.* **17**, 2007 (in press).
- [3] D. Drung, C. Hinnrichs, H.-J. Barthelmess, *Supercond. Sci. Technol.* **19**, pp. S235-S241, 2006.
- [4] D. Drung and M. Mück, in "SQUID Handbook" ed J Clark and A I Braginski (Weinheim: Wiley-VCH), pp. 127-170, 2004.
- [5] D. Drung, *Supercond. Sci. Technol.* **16**, pp1320-1336, 2003.
- [6] F. C. Wellstood, C. Urbina, and J. Clarke, *Appl. Phys. Lett.* **50**, pp. 772-774, 1987.
- [7] R. P. Welty and J. M. Martinis, *IEEE Trans. Appl. Supercond.* **3**, pp. 2605-2608, 1993.
- [8] R. Cantor, A. Hall, and V. Zotev, presented at 2nd International Workshop on Transition Edge Sensor Device Physics, Coral Gables, Florida, USA, 2004.
- [9] R. Cantor and D. Koelle, in "SQUID Handbook", Vol. I, J. Clarke and A. I. Braginski, Eds. (Weinheim: Wiley-VCH), 2004.
- [10] Manual of XXF-1 SQUID electronics, Magnicon GbR, Lemsahler landstr. 171, 22397 Hamburg, Germany, www.magnicon.com.
- [11] D. Drung and H. Koch, *IEEE Trans. Appl. Supercond.* **3**, pp. 2594-2597, 1993.
- [12] D. Drung, S. Knappe, and H. Koch, *J. Appl. Phys.* **77**, pp. 4088-4098, 1995.